JOURNAL OF AIRCRAFT
Vol. 30, No. 4, July–Aug. 1993

S-Plane Aerodynamics of Nonplanar Lifting Surfaces

Jinsoo Cho*
Pohang Institute of Science and Technology, Pohang, Republic of Korea
and
Marc H. Williams†
Purdue University, West Lafayette, Indiana 47906

A compressible unsteady panel method for predicting generalized force transfer functions for nonplanar lifting surfaces is described. The scheme is suitable for both subsonic and supersonic flow, and is valid everywhere in the complex Laplace *s*-plane. The effort of constructing the influence coefficient matrix is minimized by using the symmetry and scale properties of the kernel function. Results of steady and unsteady analyses for numerous configurations are compared with a doublet lattice method, a doublet point method, and a hybrid doublet lattice-doublet point method, showing excellent agreement. With a view toward application to rotating machinery, an analysis is given of a circular duct with guide vanes in both steady and unsteady flow.

Introduction

UNSTEADY nonplanar lifting surface methods[1-3] are routinely used in the aeroelastic analysis of aircraft to obtain the generalized aerodynamic forces resulting from vibration and gust loading. Although such methods have a long history, dating to the 1950s[4-8] papers on the subject still appear occasionally in literature.[9-12] This article describes a scheme with several novel features that has been developed as part of an effort to integrate rotating blades with the rest of the aircraft. Only the nonrotating methodology will be described here; its integration with a rotor analysis will be discussed separately. The notable features are 1) both subsonic and supersonic flows are included; 2) the formulation is valid everywhere in the complex Laplace plane; and 3) the numerical overhead of constructing the influence coefficient matrix is minimized by taking advantage of the symmetries of the unsteady kernel function. The uniform validity in the *s*-plane has applications in aeroservoelastic modeling, and to some extent removes the need for Pade (or other) curve-fitting techniques of analytic continuation from the imaginary axis (or at least allows the use of off-axis data in the curve fit). While both subsonic and supersonic flows are dealt with, any strong nonlinearities, whether of transonic, hypersonic, or high incidence origin, invalidate the model. In the interest of brevity, only subsonic results are presented here.

For steady flow, the discretization used reduces to a piecewise constant load, collocated panel method. This gives reasonable smoothness at supersonic speeds and considerable insensitivity to control point placement. However, nonsteady effects are included by a point approximation, thereby reducing the computational cost. In this latter aspect, the scheme resembles the "doublet point method" of Ueda and Dowell.[2] However, since the point approximation is applied only to nonsingular quantities, no special care need be exercised near singularities. The basic structure is such that practically any steady panel code could easily be modified for unsteady effects, simply by multiplying the influence coefficients by appropriate phase factors.

Formulation

Consider an initial value problem for linearized compressible flow in which the initial disturbances vanish away from the lifting surfaces. Taking a Laplace transform gives the usual reduced form of the equations that one gets for simple harmonic motion, but with $i\omega$ replaced by the Laplace variable s. Since the aerodynamic response (for bounded motion) should have no more than algebraic growth at large time, the Laplace integrals will be well-defined for $\mathrm{Re}(s) > 0$. We shall define the transforms in $\mathrm{Re}(s) < 0$ by analytic continuation so that the usual rules for analytic functions hold and the solutions will be meaningful in the entire s plane.

A point on a lifting surface $\boldsymbol{x}_0$ with unit normal $\boldsymbol{n}_0$ is assigned a transformed pressure differential $\Delta p = \rho UP$ acting in the direction $+\boldsymbol{n}_0$. (We will assume that $\boldsymbol{n}_0$ has no component in the freestream or x direction. The flow has speed U, density ρ, and Mach number M.) The lifting surface induces a transformed velocity (w) at an arbitrary point $\boldsymbol{x}$, in an arbitrary direction $\boldsymbol{n}$, which is given by an integral over the lifting surface:

$$w(\boldsymbol{x}) = \int\int K(\boldsymbol{x}, \boldsymbol{x}_0) P(\boldsymbol{x}_0)\, \mathrm{d}A_0 \tag{1}$$

The kernel K is the fundamental solution of the reduced wave equation corresponding to the velocity w induced at $\boldsymbol{x}$ by a point load applied at $\boldsymbol{x}_0$. Its properties will be discussed later. In the standard problem, w is specified on the surface and we solve for the load P, though in some design applications we may simply evaluate w given P. In either case the integral is discretized, for simplicity, by a piecewise constant approximation

$$w = CP \tag{2}$$

where C is the integral of K over each subdomain (or panel), and $\boldsymbol{P}$ is to be thought of as a vector of loads on all panels. The problem then is to develop efficient methods for evaluating the coefficients C, with accuracy consistent with the discretization errors in Eq. (2). It is not efficient to evaluate the elements of C exactly, because of the complexity of the kernel function.

The kernel K can be abbreviated as

$$K = \bar{K}_p K_0 + D\boldsymbol{n}_0 \cdot \boldsymbol{\xi} K_{p_0} \tag{3}$$

where $\boldsymbol{\xi} = (y - y_0)\boldsymbol{j} + (z - z_0)\boldsymbol{k}$. The quantities K_{p_0} and K_0 are the steady-state planar and nonplanar kernels, respectively. These functions are singular on the axis $\xi = 0$, $X > 0$. In supersonic flow, they are also singular on the Mach cone. The factor $\bar{K}_p$ is the ratio of the unsteady to steady

Received Jan. 2, 1992; revision received May 14, 1992; accepted for publication May 14, 1992.

*Assistant Professor, Department of Mechanical Engineering and Advanced Fluids Engineering Research Center. Member AIAA.
†Professor, School of Aeronautics and Astronautics. Member AIAA.

planar kernels. The coefficient D is given in terms of derivatives of $\bar{K}_p$

$$D = \boldsymbol{n}\cdot\left(i\frac{\partial}{\partial X} + \boldsymbol{\xi}\frac{1}{\xi}\frac{\partial}{\partial \xi}\right)\bar{K}_p \tag{4}$$

where $X = x - x_0$. Note that in steady flow, $\bar{K}_p = 1$ and $D = 0$. The significant point is that $\bar{K}_p$ is a regular function (i.e., has no singularities) and so can be treated as nearly constant over each panel, while its derivatives can be evaluated by finite differences. Therefore, the influence coefficient C is approximated by

$$C = \bar{K}_p C_0 + DC_{p_0} \tag{5}$$

where C_0 and C_{p_0} are the nonplanar and planar steady influence coefficients, respectively, which can be evaluated analytically (see Appendix.) The unsteady factors $\bar{K}_p$ and D are evaluated at only one point on the panel. It should be noted that this splitting off by factorization of the unsteady part of the kernel is the distinguishing feature of the present scheme. It is more common to split by subtraction.

Before defining $\bar{K}_p$ in detail, it should be noted that it depends only on relative axial and radial separations X and ξ, as well as the Mach number and the scaled complex Laplace variables $\bar{s} = s/U$. Since the function is nondimensional, it must depend only on the products $\bar{s}X$ and $\bar{s}\xi$ (of which it must be a real function). In the current work we take it to be

$$\bar{K}_p = \bar{K}_p(sx, sy; M, \Phi) \tag{6}$$

where $sx = |\bar{s}|X$ and $sy = |\bar{s}|\xi$, and Φ is the argument of $\bar{s}$. The range of sx and sy are set by the largest desired magnitude of $\bar{s}$ and the geometry of the body. This range is determined a priori, and the function $\bar{K}_p$ is then tabulated on a rectangular grid covering that range, with a grid density which is somewhat finer than the resolution of the paneling that is to be used. Values of $\bar{K}_p$ and its derivatives are then found by interpolation in the table when the influence coefficient matrix is computed. The advantage of this scheme is that the number of kernel evaluations scales with the number of panels, rather than the square of the number of panels as would be the case if the evaluations were done as needed. Furthermore, the table does not need to be reconstructed for any values of $\bar{s}$ with smaller magnitude than that used to define the table. The table is reconstructed only when M, Φ, or the geometry is modified. (Clearly, since Gaussian elimination scales as the cube of the number of panels, minimizing matrix setup cost will payoff only for moderate-sized problems. Construction of the table is sensible only when many solutions with given M, Φ, and geometry are needed.)

Neglecting the variation of $\bar{K}_p$ over a panel requires that the panel widths should be small compared to the "wavelength," $1/|\bar{s}|$. This clearly means that finer discretization is necessary when $|s|$ increases. The present scheme would not be optimal for extremely large frequencies. For convenience, the point of evaluation of the unsteady factors has been set at the panel centroid. A better choice is the centroid of the generalized area $K_{p_0}\,dA$, which would reduce the quadrature error, especially for a panel containing singularities, but which would also make the evaluation point vary with control point location.

The panels are constructed as quadrilaterals with side edges parallel to the flow. The control points are fixed along the midspan, at 85% local chord. This choice optimizes subsonic convergence rate with panel refinement (this is most easily seen for two-dimensional steady flow, for which the exact solution of the Cauchy integral equation is known). The scheme is convergent for any control point placement downstream from the panel midchord. If control points were placed toward the leading edge, subsonic solutions would appear to satisfy a Kutta condition at the leading, rather than the trailing edge. (This is exactly so for two-dimensional steady flow, where the kernel is antisymmetric. For three-dimensional unsteady flow, where the kernel is asymmetric, the solutions obtained with the control point in front of midchord are, more exactly, wrong.) The control point placement seems to be irrelevant for supersonic flow with supersonic edges.

Kernel Function

In this section the kernel function introduced in Eq. (3) is defined. Let λ be 0 if $M < 1$ and 1 if $M > 1$. The steady planar kernel is

$$K_{p_0} = \Lambda/(4\pi R) \tag{7}$$

where

$$R^2 = X^2 + \beta\xi^2$$
$$\beta = 1 - M^2$$
$$\Lambda = [(1 + \lambda)X + (1 - \lambda)R]/\xi^2$$

When $M < 1$ and $X < 0$ it is better to use the equivalent expression, $\Lambda = \beta/(R - X)$, which is regular at $\xi = 0$.

The nonplanar steady kernel can be expressed simply as

$$K_0 = \boldsymbol{n}\cdot\nabla(\boldsymbol{n}_0\cdot\boldsymbol{\xi}K_{p_0}) \tag{8}$$

The supersonic kernel is, of course, defined as 0 for any point outside the downstream Mach cone from the load point.

The unsteady factor $\bar{K}_p$ is

$$\bar{K}_p = E/\Lambda[M(E^- + \lambda E^+) + RB] \tag{9}$$

where

$$E = \exp(-\bar{s}X)$$
$$E^{\pm} = \exp(\bar{s}\zeta^{\pm})/R^{\pm}$$
$$R^{\pm} = \mathrm{sqrt}[\xi^2 + (\zeta^{\pm})^2]$$
$$\zeta^- = (X - MR)/\beta$$
$$\zeta^+ = \begin{cases} (X + MR)/\beta & \text{if } M > 1 \\ -\infty & \text{if } M < 1 \end{cases}$$
$$B = \int_{\zeta^+}^{\zeta^-} \exp(\bar{s}v)/(v^2 + \xi^2)^{3/2}\,dv \tag{10}$$

Although $\bar{K}_p$ is nonsingular, it does need special treatment along certain lines of removable singularity. Specifically, $\bar{K}_p = E$ on $\xi = 0$, $X > 0$. Furthermore, in supersonic flow, the definition outside the downstream Mach cone is somewhat arbitrary. To maintain some continuity for panels which straddle the Mach cone, we take $\bar{K}_p = \exp(\bar{s}XM^2/\beta)$ at all points outside the Mach cone (this being the value on the cone at the same X). This eliminates sensitivity to whether the evaluation point on the panel happens to fall just within, or just without, the zone of dependence of the control point. One difficulty with the scheme for high-frequency supersonic flow (which does not arise if $M < 1$) is that for large $\bar{s}X$ a boundary-layer thickness of $\Delta\xi = O(1/|\bar{s}|)$ develops on the interior face of the Mach cone. Outside the boundary layer, $\bar{K}_p$ varies on the scale $\xi = O(X)$. Resolving the boundary layer can require an inordinately large number of panels.

Note that $\bar{K}_p$ is continuous everywhere in the complex s-plane when $M > 1$. However, for $M < 1$, the quantity B as defined in Eq. (10) is meaningful only for $\mathrm{Re}(s) > 0$. To define B, and therefore the solution, in $\mathrm{Re}(s) < 0$ for subsonic flow, we make use of a simple analytic continuation. Let $B(a1, a2)$ denote the integral with lower and upper limits $a1$ and $a2$. Clearly, then

$$B(-\infty, \zeta^-) = B(-\infty, -b) + B(-b, \zeta^-) = B_0 + B_1$$

where b is any positive real number, and B_0 and B_1 are the infinite and finite parts, respectively. The second term, B_1 is analytic but the first term, B_0 is not defined in $\mathrm{Re}(s) < 0$. Since B_0 has real support, it is sufficient to consider its continuation for $\mathrm{Im}(s) > 0$. The integrand has a branch cut along $-\xi < \mathrm{Im}(v) < \xi$ on the imaginary v axis, and vanishes exponentially in the left-half v plane. Therefore, as long as $b > 0$, the integration path can be turned from $(-\infty, -b)$ to $(-b, +i\infty)$. The result is

$$B_0 = \int_0^\infty \exp(-\chi)\, dr \tag{11}$$

where

$$\chi = (b - ir)\bar{s} + 1.5\, \ell n\, A + i(\pi - 3\theta)/2$$
$$A = [(b^2 + \xi^2 - r^2)^2 + (2br)^2]^{0.5}$$
$$\theta = \cos^{-1}[(b^2 + \xi^2 - r^2)/A]$$

The function B_0 defined by Eq. (11) is identical to Eq. (10) in $\mathrm{Re}(s) > 0$, $\mathrm{Im}(s) > 0$, but is analytic in the entire upper half-plane, $\mathrm{Im}(s) > 0$. Since values in $\mathrm{Im}(s) < 0$ can be obtained by conjugation, Eq. (11) serves as the desired continuation of B_0 into the entire complex s plane. It has a simple branch cut along the negative real axis, but it is continuous elsewhere.

Note that B_0 is a function only of radius ξ, and so can be computed and stored once over the range of possible radii. [From Eq. (6), it is sufficient to compute B_0 for $|\bar{s}| = 1$.] Values for specific panel and control point combinations are obtained by interpolation. The constant b is chosen to be approximately ξ_{max}, the largest radius of the configuration. All integrals (B_0 and B_1 in subsonic or B in supersonic flow) are computed by numerical quadrature, using a scheme that is exact for $s = 0$.

Results

Comparison with Doublet Lattice Method

The present method was first validated by comparing it with the results of a doublet lattice calculation by Kalman et al.[13] Figure 1 compares the lift-curve slope C_{L_α} calculated by the present method, and by the doublet lattice method (DLM) for wings with dihedral angle γ at various heights h above a ground plane. The wing has a rectangular planform with aspect ratio 4.0 and chord c, and is in steady incompressible flow. The wing half-plane was discretized with 8 chordwise and 10 spanwise panels, and the ground effect was included by images. The two calculations show almost identical results for this classical problem.

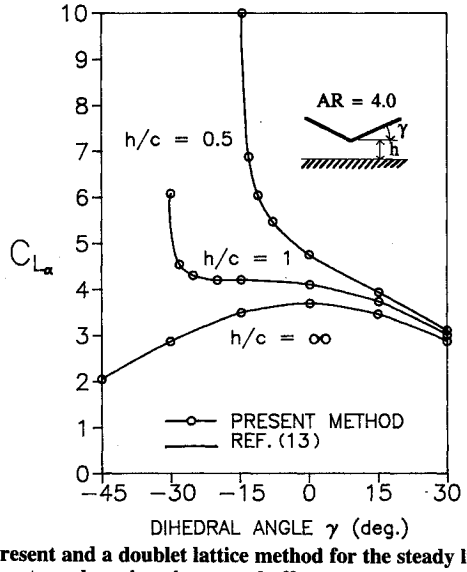

Fig. 1 Present and a doublet lattice method for the steady lift-curve-slope for rectangular wings in ground effect.

The second example is an annular wing which has been analyzed by Belotserkovskii[16] using slender wing theory. As shown in Fig. 2, the annulus has various diameter to length ratio D/L. The ring is divided into 24 circumferential and 10 chordwise (streamwise) panels as in Ref. 13. Figure 2 shows a comparison of 1) static stability derivatives, 2) lift-curve-slope, 3) pitching moment, and 4) pitch rate coefficients (about the midchord) as calculated by Belotserkovskii's slender wing theory, by the doublet lattice method, and by the present method. Except for the slender wing theory at large D/L, the three calculations are in close agreement.

Calculations were made as well for the annulus undergoing harmonic pitching motion with unit amplitude at a low reduced frequency $k = \omega L/2U = 0.05$, where ω and U represent angular frequency and freestream velocity, respectively. Figure 3 shows the pitch rate stability derivatives for 1) $C_{L_{\dot\alpha}}$, and 2) $C_{M_{\dot\alpha}}$ (see Ref. 17), calculated by the present method and by DLM. The two methods agree as well as in the steady case. Figure 3 also shows the results of the slender wing theory of Laschka.[14]

To demonstrate the capability of the present method in handling the interference of intersecting multiple lifting surfaces, steady and unsteady results of a wing with pylons are compared in Fig. 4 in terms of sectional lift curve slope (c is

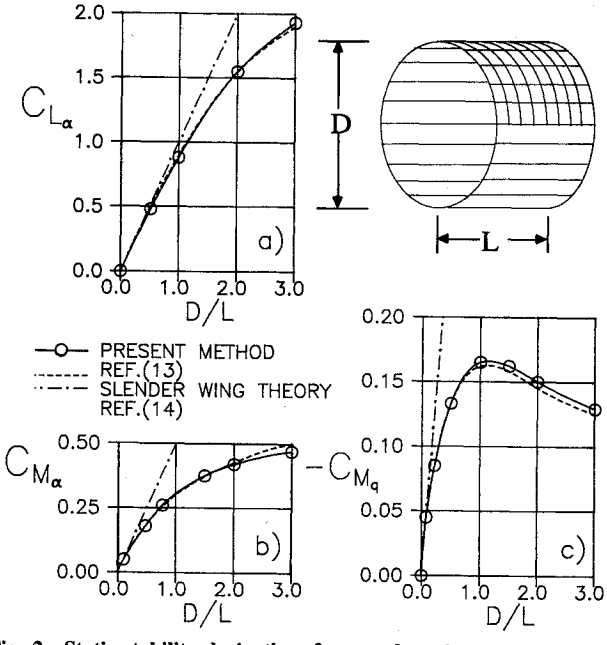

Fig. 2 Static stability derivatives for annular wings of various D/L ratios.

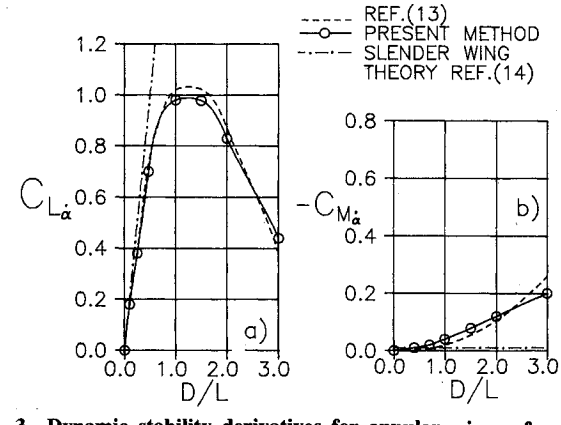

Fig. 3 Dynamic stability derivatives for annular wings of various D/L ratios.

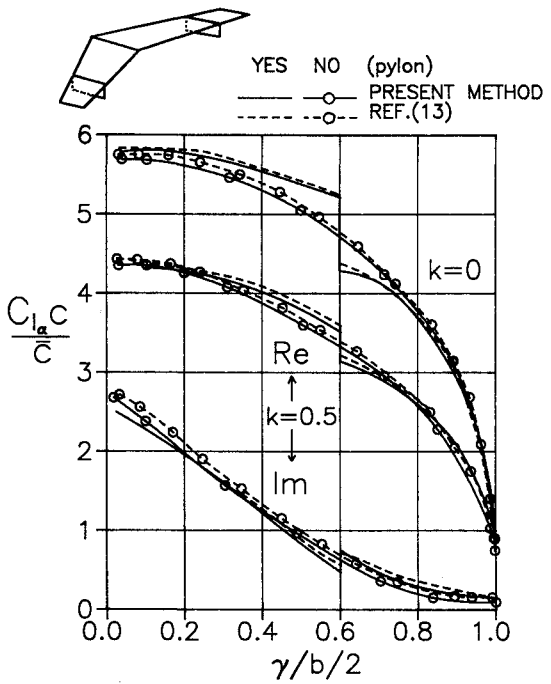

Fig. 4 Sectional lift-curve-slopes for a wing with and without pylons in steady and unsteady flow.

Table 1 Generalized forces as calculated by the present and double point method; $\eta = -0.4 + 0.4i$, $M = 0.8$.

	DMP by Ueda[15]	Present method
q_{11}	$-1.6756 + 0.0332i$	$-1.7183 - 0.1001i$
q_{21}	$-0.5075 + 0.0002i$	$-0.5231 - 0.0383i$
q_{31}	$1.1984 - 2.1201i$	$1.2051 - 2.0441i$
q_{41}	$0.3296 - 0.6335i$	$0.3444 - 0.6219i$
q_{12}	$-0.5075 + 0.0002i$	$-0.5231 - 0.0383i$
q_{22}	$-0.2000 - 0.0155i$	$-0.2052 - 0.0281i$
q_{32}	$0.3460 - 0.6394i$	$0.3620 - 0.6248i$
q_{42}	$0.1353 - 0.2294i$	$0.1363 - 0.2290i$
q_{13}	$0.9375 + 4.1731i$	$0.5321 + 4.3031i$
q_{23}	$0.2886 + 1.2734i$	$0.1707 + 1.3211i$
q_{33}	$-6.2170 + 0.0617i$	$-6.1028 - 0.2354i$
q_{43}	$-1.8439 + 0.1171i$	$-1.8369 + 0.0409i$
q_{14}	$0.3050 + 1.2675i$	$0.1884 + 1.3183i$
q_{24}	$0.0930 + 0.4993i$	$0.0564 + 0.5167i$
q_{34}	$-1.8717 + 0.1039i$	$-1.8601 + 0.0220i$
q_{44}	$-0.6823 + 0.0690i$	$-0.6864 + 0.0551i$

the sectional chord length and $\bar{c}$ the average chord.) The wing has an aspect ratio of 6.67, a taper ratio of 0.33, and a quarter chord sweepback angle of 30 deg. The Mach number is low. The rectangular pylon lies along the chord at 60% semispan with height equal to 20% of the wing semispan. The half-wing is discretized with 14 panels distributed nonuniformly along the span (dense near the pylon) and 6 uniformly placed along the chord. The pylon has six uniform strips vertically with the same chordwise partition as the wing. The comparison for the two methods is made with and without the pylon, for both steady state ($k = 0$) and dynamic pitch about the wing apex at $k = 0.5$. The two methods give basically the same results for all the cases examined. Comparisons with experimental measurements were shown in Ref. 13 and will not be reproduced here.

Comparison with Doublet Point Method

The Laplace domain capability of the present method was tested by comparing it with the results presented by Ueda[15] for the generalized forces on a flexible rectangular wing. That calculation employed the doublet point method (DPM) developed earlier by Ueda and Dowell.[2] Table 1 compares the generalized forces, (q_{ij}) defined as

$$q_{ij}(\eta) = \int \int_{\text{wing}} h_i(x, y) P_j(x, y)\, dx\, dy$$

for four deflection modes (h_i) given by

$$h_1 = 1 \qquad \text{(heaving)}$$

$$h_2 = 1.2(y/3)^2 - 0.2(y/3)^4 \qquad \text{(bending)}$$

$$h_3 = x - 1 \qquad \text{(pitching)}$$

$$h_4 = (x - 1)[1.2(y/3)^2 - 0.2(y/3)^4] \qquad \text{(torsion)}$$

where (x, y) are streamwise and spanwise coordinates measured in semichords, b; P_j is the load resulting from mode j vibration; and $\eta = bs/U$ is the normalized Laplace transform variable s.

The wing has an aspect ratio of 3 and the half-surface was discretized with 10 chordwise and 20 spanwise elements. The Mach number is 0.8 and the Laplace parameter lies in the stable half-plane (where analytic continuation of the kernel is crucial), $\eta = -0.4 + 0.4i$ as in Ref. 15.

The two sets of generalized derivatives listed in Table 1 are in close agreement in magnitude, but in some cases there are large relative differences in the smaller part of the complex amplitude (real or imaginary). The agreement in magnitude suggests the validity of the two analytic continuations employed. The large relative differences in the small parts is a result of the differing truncation errors of the two schemes with the same paneling. If these subdominant parts are important, a finer paneling may be necessary.

Comparison with the Hybrid Doublet Lattice-Doublet Point Method

Eversman and Pitt[11] developed a hybrid doublet lattice-doublet point method to overcome the shortcomings of the doublet point method of Ueda and Dowell[2] for modeling aerodynamic strips of unequal width and nonplanar lifting surfaces, while retaining its computational efficiency in the far field. The present method was compared with hybrid method results obtained from Ref. 11 for the two unsteady cases of a rectangular wing and a tapered swept wing. Figure 5 shows the sectional lift curve slopes by the hybrid scheme and the present method for a rectangular wing an aspect ratio of 4.0 pitching about the $\frac{1}{4}$ chord at a Mach number of 0.8 and a reduced frequency (k) of 0.3. The half-span panel discretization is indicated in this figure. The detailed planform of the tapered and swept wing is shown in Fig. 6. The wing undergoes harmonic rigid rotation about an axis at $\frac{1}{2}$ chord, with Mach number 0.8 and reduced frequency $k = 0.5$. Figure 6 shows good agreement between the sectional lift distributions computed from the two methods.

Ducted Vane

One of the purposes of developing the present method was to apply it to the unsteady aerodynamic and aeroelastic anal-

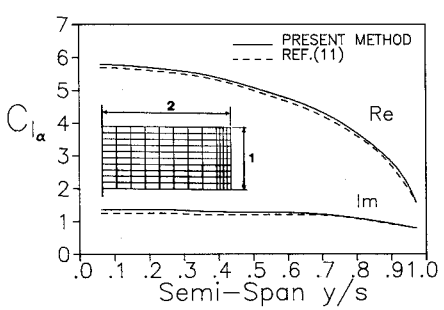

Fig. 5 Unsteady sectional lift on a rectangular wing oscillating in pitch about the $\frac{1}{4}$ chord; $M = 0.8$, $k = 0.3$, as calculated by the present method and a hybrid doublet lattice-doublet point method.

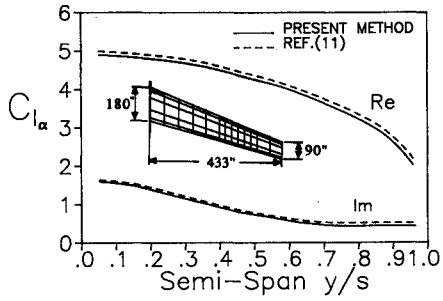

Fig. 6 Unsteady sectional lift of a high aspect ratio swept wing in rigid pitch about the midchord; $M = 0.8$, $k = 0.5$, as calculated by the present method and a hybrid doublet lattice-doublet point method.

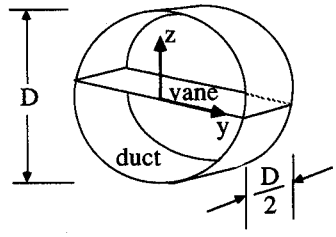

Fig. 7 Simplified ducted van configuration.

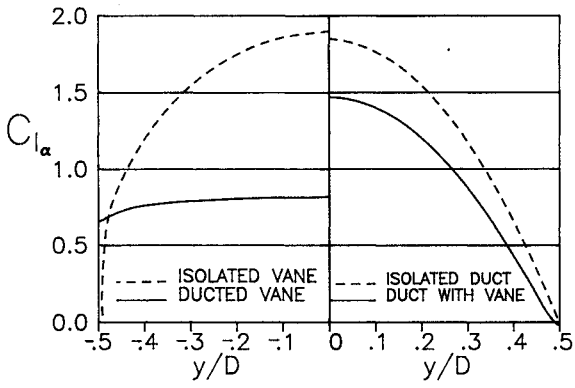

Fig. 8 Sectional lift on vane/duct configurations in steady incompressible flow.

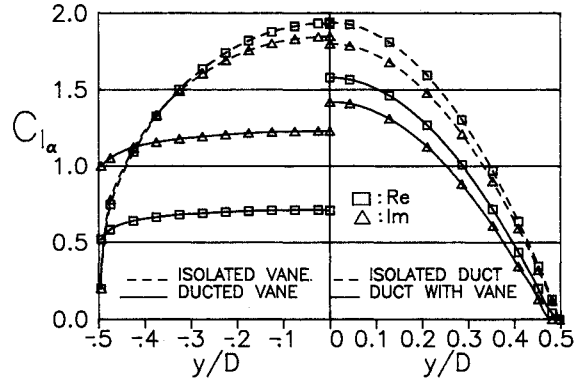

Fig. 9 Sectional lift on vane/duct for the harmonic pitching motion about the midchord; $M = 0.5$, $k = 0.5$.

ysis of ducted fans with guide vanes. The authors have shown results for the aerodynamic analysis of propeller-wing interaction and counter-rotating propellers systems in Ref. 12 and Ref. 18, respectively. An analysis of ducted fans without guide vanes has been already developed.[19]

The ability of the present method to model guide vanes inside a duct (without fan) was tested for the simplified ducted vane configuration shown in Fig. 7. Figure 8 compares the sectional steady lift due to angle of attack plotted vs span, for three configurations: 1) vane without duct, 2) duct without vane, and 3) combined duct and vane. The vane loads are shown on the left, the duct loads on the right. It can be clearly seen that the presence of the duct lowers the vane lift significantly, and the presence of the vane inside the duct affects the duct only moderately. (The signs and magnitudes of these effects can easily be estimated from consideration of a stack of three airfoils. The results shown agree with these estimates.) A similar comparison is made in Fig. 9 for the case when the assembly undergoes harmonic pitch about the midchord at a reduced frequency (based on semiduct length) of 0.5.

The duct was discretized with 36 circumferential and 10 chordwise panels, and the vane with 20 spanwise and 10 chordwise panels. The symmetry properties of the kernel function were not used. Total computing time for the steady results of Fig. 8 and unsteady results of Fig. 9 using SUN Sparc 4/75 work station, were 9 and 18 min, respectively.

Conclusion

A new nonplanar, unsteady, lifting surface scheme has been presented which is conceptually simple, in that the unsteady influence coefficients are obtained by multiplying the steady influence coefficients by frequency-dependent phase factors. The new method has been verified by showing that it produces results that are in excellent agreement with published results of other lifting surface methods, in particular, double lattice, point doublet, and a hybrid of the two. Although the actual computing times could not be compared for each case, the present frequency domain calculation is only marginally more expensive than a pure steady-state panel method. It is applicable to both subsonic and supersonic flows, though only subsonic results were presented herein. The scheme is based on a uniformly valid analytic continuation of the unsteady kernel function in the complex Laplace plane, so it is usable for any complex s (except negative reals, where there is a branch cut).

The results for the annular wing proved that the present method can be used for predicting both static and dynamic stability derivatives. Although experimental data were not available for the cases examined, such comparisons were made in Ref. 13 using the doublet lattice method, and similar agreement should be expected here.

The comparisons made with the doublet point method show that the present method can be used for forced vibration and flutter prediction. It is important to note that the present scheme is not restricted to planar lifting surfaces, as was the earlier scheme.

Both steady and unsteady results for a simplified ducted vane model showed the possibility of analyzing ducted fans with guide vanes when the present method is integrated with a rotating lifting surface method the authors have previously developed, and applied to the aerodynamic and aeroelastic analysis of ducted fans without guide vanes.

Appendix

For the sake of completeness, formulas for the steady-state influence coefficients are given here. The panels are assumed to be quadrilateral with sides parallel to the flow (X) direction. The following results are in local panel coordinates (X, Y, Z), measured from the control point, with Z normal to the panel

$$C_0 = \Delta_x \Delta_y \boldsymbol{n} \cdot \boldsymbol{F}/(4\pi)$$

$$C_{p_0} = \Delta_x \Delta_y F_0/(4\pi)$$

where Δ_x and Δ_y denote difference operators between corner points in the respective directions. The four quantities F and F_0 are

$$F_x = (1 + \lambda)\tan^{-1}[(m\xi^2 - XY)/(RZ)]$$

$$F_y = -mF_x + Z\Lambda$$

$$F_z = mF_x^r - (1 + \lambda)\hat{a}^2 G_1 - Y\Lambda$$

$$F_0 = XF_x + YF_y + ZF_z$$

where

$$m = \Delta_x X/\Delta_y Y$$

$$\hat{a}^2 = m^2 + \beta$$

$$\varepsilon = \{|\beta|[\hat{a}^2 Z^2 + (X - mY)^2]\}^{1/2}$$

$$F_x^r = -(1 + \lambda)\,\ell n\,|(R + X)/(R - X)| + (1 - \lambda)\,\ell n\,\xi$$

Finally, with $\zeta = (mX + \beta Y)$

$$G_1 = (0.5/\hat{a})\,\ell n\,|(R - \zeta/\hat{a})/(R + \zeta/\hat{a})| \quad \text{for} \quad \hat{a}^2 > 0$$

$$G_1 = \sin^{-1}(\zeta/\varepsilon)/|\hat{a}| \quad \text{for} \quad \hat{a}^2 < 0$$

References

[1]Hammond, C. E., Runyan, H. L., and Mason, J. P., "Application of Unsteady Lifting Surface Theory to Propellers in Forward Flight," AIAA Paper 74-419, April 1974.

[2]Ueda, T., and Dowell, E. H., "A New Solution Method for Lifting Surfaces in Subsonic Flow," *AIAA Journal*, Vol. 20, No. 3, 1982, pp. 348–355.

[3]Appa, K., "Constant Pressure Panel Method for Supersonic Unsteady Airload Analysis," *Journal of Aircraft*, Vol. 24, No. 10, 1987, pp. 696–702.

[4]Landahl, M. T., "Kernel Function for Nonplanar Oscillating Surfaces in a Subsonic Flow," *AIAA Journal*, Vol. 5, No. 5, 1967, p. 1045.

[5]Landahl, M. T., and Stark, V. J. E., "Numerical Lifting-Surface Theory Problems and Progress," *AIAA Journal*, Vol. 6, No. 11, 1968, pp. 2049–2060.

[6]Albano, E., and Rodden, W. P., "A Doublet-Lattice Method for Calculating Lift Distributions on Oscillating Surfaces in Subsonic Flows," *AIAA Journal*, Vol. 7, No. 2, 1969, pp. 279–285.

[7]Rodden, W. P., Giesing, J. P., and Kalman, T. P., "Refinement of the Nonplanar Aspects of the Subsonic Doublet-Lattice Lifting Surface Method," *Journal of Aircraft*, Vol. 9, No. 1, 1972, pp. 69–73.

[8]Brune, G. W., and Dusto, A. R., "Slowly Oscillating Lifting Surfaces at Subsonic and Supersonic Speeds," *Journal of Aircraft*, Vol. 9, No. 11, 1972, pp. 777–783.

[9]Miyazawa, Y., and Washizu, K., "A Finite State Aerodynamic Model for a Lifting Surface in Incompressible Flow," *AIAA Journal*, Vol. 21, No. 2, 1983, pp. 163–171.

[10]Katz, J., and Maskew, B., "Unsteady Low-Speed Aerodynamic Model for Complete Aircraft Configurations," *Journal of Aircraft*, Vol. 25, No. 4, 1988, pp. 302–310.

[11]Eversman, W., and Pitt, D. M., "A Hybrid Doublet Lattice-Doublet Point Method for Complete Aircraft Configurations," AIAA Paper 89-1322, April 1989.

[12]Cho, J., and Williams, M. H., "Propellar-Wing Interaction Using a Frequency Domain Panel Method," *Journal of Aircraft*, Vol. 27, No. 3, 1990, pp. 196–203.

[13]Kalman, T. P., Rodden, W. P., and Giesing, J. P., "Application of the Doublet-Lattice Method to Nonplanar Configurations in Subsonic Flow," *Journal of Aircraft*, Vol. 8, No. 6, 1971, pp. 406–413.

[14]Laschka, B., "Uber die Potentialtheorie von zylindrischen rotationssymmetrischen Flugeln (Ringflugel) in kompressibler instationarer Unterschallstromung," Zeitschrift fur Flugwissenschaften, Band 12, Heft 6, 1964, pp. 205–211.

[15]Ueda, T., "Lifting Surface Calculations in the Laplace Domain with Application to Root Loci," *AIAA Journal*, Vol. 25, No. 5, 1987, pp. 698–704.

[16]Belotserkovskii, S. M., "The Theory of Thin Wings in Subsonic Flow," Plenum Press, New York, 1967.

[17]Rodden, W. P., and Giesing, J. P., "Application of Oscillatory Aerodynamic Theory for Estimation of Dynamic Stability Derivatives," *Journal of Aircraft*, Vol. 7, No. 3, 1970, pp. 272–275.

[18]Cho, J., and Williams, M. H., "Counter Rotating Propeller Analysis Using a Frequency Domain Panel Method," *Journal of Propulsion and Power*, Vol. 6, No. 4, 1990, pp. 426–433.

[19]Williams, M. H., Cho, J., and Dalton, W. N. "Unsteady Aerodynamic Analysis of Ducted Fans," *Journal of Propulsion and Power*, Vol. 7, No. 5, 1991, pp. 800–805.